IEEE Access
Multidisciplinary | Rapid Review | Open Access Journal

Received June 25, 2021, accepted July 22, 2021, date of publication August 9, 2021, date of current version August 25, 2021.

Digital Object Identifier 10.1109/ACCESS.2021.3103763

Beats-to-Beats Estimation of Blood Pressure During Supine Cycling Exercise Using a Probabilistic Nonparametric Method

QING LIU[1], (Member, IEEE), YALI ZHENG[2], (Member, IEEE), YUANTING ZHANG[3], (Fellow, IEEE) AND CARMEN C. Y. POON[4], (Senior Member, IEEE)

[1]School of Advanced Technology, Xi'an Jiaotong–Liverpool University, Suzhou, Jiangsu 215123, China
[2]College of Health Science and Environmental Engineering, Shenzhen Technology University, Shenzhen, Guangdong 518118, China
[3]Department of Mechanical and Biomedical Engineering, City University of Hong Kong, Hong Kong
[4]GMed IT, Ltd., Hong Kong

Corresponding author: Carmen C. Y. Poon (cpoon@link.cuhk.edu.hk)

This work was supported in part by Hong Kong General Research Fund, Hong Kong Innovation and Technology Fund, Natural Science Foundation of Jiangsu Higher Education Institutions of China, under Grant 18KJB416007, in part by Shenzhen Fundamental Research Program under Grant JCYJ20190813111001769, in part by Guangdong Province High Education Young Innovative Talent under Grant 2019KQNCX178, and in part by the Natural Science Foundation of Top Talent of SZTU under Grant 2020110.

This work involved human subjects or animals in its research. Approval of all ethical and experimental procedures and protocols was granted by the Joint Chinese University of Hong Kong-New Territories East Cluster Clinical Research Ethics Committee, and performed in line with the Declaration of Helsinki.

ABSTRACT Blood pressure (BP) is an important clinical vital sign that varies from beat-to-beat. Nevertheless, these variations cannot be captured by the conventional cuff-based BP monitors. This study proposes and evaluates novel cuffless frameworks to continuously estimate the 10-beat averaged systolic BP (SBP) and diastolic BP (DBP) during dynamic exercise by fusing information from multiple biosensors using five machine learning algorithms. Over 100 thousand beats of data were collected from 62 subjects (aged 59 ± 10 years), each underwent a maximal exercise stress test. The average length of recording for each subject was 35 minutes. The BP ranges were 75-280 mmHg for SBP and 36-157 mmHg for DBP respectively. Multiple physiological parameters were measured continuously and used as inputs to five machine learning algorithms for estimating the 10-beat SBP and DBP averages before, during and after the cycling exercise. The mean absolute error (MAE) of Gaussian process regression (GPR) model was 4.8 mmHg and 3.4 mmHg for SBP and DBP, respectively. The MAE of multiple linear regression (MLR), regression tree (RT), ensemble of trees (ETs), and support vector machine (SVM) models varied from 6.1 mmHg to 17.6 mmHg and from 4.0 mmHg to 9.7 mmHg for SBP and DBP, respectively. The GPR model outperformed the other four models and showed promising results in estimating the 10-beat averages of both SBP and DBP without a cuff in a general elderly population under dynamic conditions.

INDEX TERMS AI-doscopist, cuffless blood pressure, machine learning, big data analytics, wearable sensing, sensor network.

I. INTRODUCTION

Hypertension remains one of the leading causes to global morbidity and mortality for over half a century [1]. Hypertension is treatable by improving awareness of lifestyle and promoting health behaviors. Diagnosis rate of hypertension is, however, as low as 46%, and only about a third of those diagnosed are adequately controlled [2].

The associate editor coordinating the review of this manuscript and approving it for publication was S. M. Rezaul Hasan.

According to the Systolic Blood Pressure Intervention Trial (SPRINT) [3], ambulatory blood pressure (BP) monitoring will help improve the awareness and management of hypertension. Nevertheless, existing ambulatory BP monitors are mostly developed by the oscillometric approach, which operates based on the inflation and deflation of a brachial cuff. These devices can only provide a snapshot of BP. Although continuous BP can be obtained noninvasively by tonometry and volume-clamp methods, these methods are relatively cumbersome. Tonometry requires frequent calibration

as well as applanating the artery using a probe which has been proven difficult; while volume-clamp methods used inflatable cuffs in the design and are disruptive during ambulatory monitoring, especially during sleeping [4]. A recent study developed a smartphone-based device based on the oscillometric technique for cuff-less and calibration-free monitoring of BP, however, it can hardly be applied to long-term continuous BP or nighttime BP measurements as it requires human finger pressing during measurement [5].

Alternatively, pulse transit time (PTT) or its reciprocal – pulse wave velocity (PWV) has been investigated extensively as a surrogate of BP for continuous and wearable cuff-less BP measurement over a decade [6]. PTT is the time delay for a pressure wave to propagate between two arterial sites (typically between a proximal site and a distal site). Governed by the wave propagation theory, PWV is determined by the arterial elasticity which depends on BP. Thus, PTT is inversely related to BP mathematically. PTT can be estimated from different biosensors, e.g. electrical, optical, mechanical, bioimpedance, magnetic and radar [4]. In practice, one of the most widely used methods for PTT measurement (i.e., pulse arrival time, PAT) is by calculating the time interval between the R-peak of the electrocardiogram (ECG) and a characteristic point (i.e. foot or peak) of the peripheral photoplethysmography (PPG) in the same cardiac cycle. PAT contains a pre-ejection period (PEP), which is a confounding factor influencing relationship between PAT and BP [7], [8]. Nevertheless, PAT methods are still commonly used for cuff-less BP estimation attributed to its great convenience.

The BP-PTT relationship depends on the mechanical property of the arterial wall comprising elastin, collagen fibers and smooth muscle cells (SMCs). Innervated by the autonomic nervous system (ANS) and regulated by the neuro-humoral factors, SMCs can actively contract/dilate to alter the elasticity of arterial wall and the BP-PTT relationship. Therefore, vascular tone which represents the activation level of SMCs, is another essentially important factor that influences PTT-based BP estimation in addition to PEP. Our previous study showed that PTT can be used to estimate 24-hour ambulatory blood pressure [9], but clearly demonstrated a hysteresis phenomenon against SBP during dynamic exercise [10]. It was recently suggested that this is partly because the derivations based on the Moens–Korteweg (MK) and Hughes equations relied on assumptions that do not hold for human arteries and that the artery hyperelastic model should be used to describe the relationship between BP and PWV [11]. Moreover, as peripheral arteries contain more smooth muscles than central arteries, these influences become even more prominent when using peripheral pulses to calculate PTT or PAT [4].

Although biophysical models were important to understand the basic underlying mechanism, these models often felt short in describing the system under a complex situation when the parameters of different submodules were interrelated and the relationship between different submodules were not completely known. On the other hand, a recent direction is to incorporate machine learning (ML) techniques and pulse wave analysis for BP estimation [12]. In particular, since the waveform of a peripheral pulse obtained by PPG depend on multiple factors of the cardiovascular system, such as BP, contractile force of the heart, and elasticity of the arterial wall [13], PPG waveform features have been often used together with PTT for estimating BP using ML techniques. Various ML regression techniques have been investigated [14]–[17], nevertheless, most of these studies were conducted in static conditions, while studies on estimating BP in dynamic conditions, e.g. during exercise when BP of each subject varied greatly, were quite limited.

In this study, we aim to evaluate novel frameworks to estimate beats-to-beats SBP and DBP by fusing information from multiple biosensors using five ML techniques: multiple linear regression (MLR), regression tree (RT), ensemble of trees (ETs), support vector machine (SVM) and Gaussian process regression (GPR). Specifically, we focused on the complex relationship between BP and features from wearable sensors (i.e. PTT and PPG waveform features) on elderly subjects during maximal exercise stress test. The physiological conditions was chosen based on the fact that abnormal BP responses during and after exercise are associated with heightened cardiovascular risk that may be unnoticed by conventional resting BP screening methods. In addition to its prognostic value, continuous monitoring of BP during exercise is also desirable as it can be important external trigger of cardiovascular events, especially in elderlies whose arteries are often stiffer and less able to absorb BP surges [18].

II. METHODOLOGY

A. SUBJECTS

Sixty-two subjects (aged 59 ± 10 years) participated in the experiment. Amongst them, 22 were healthy, 16 were with different cardiovascular risk factors (i.e., hypertension), and 24 were diagnosed with different CVDs, demonstrating large differences in CVD status in the population. Figure 1 shows the clinical characteristics of these subjects. The study was approved by the Joint Chinese University of Hong Kong – New Territories East Cluster Clinical Research Ethics Committee. Each subject signed the informed consent before participating in the experiment.

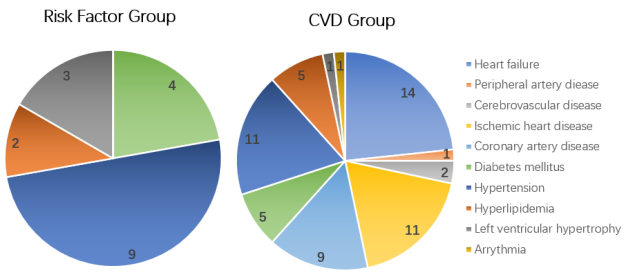

FIGURE 1. Clinical characteristics of the subjects participated in this study.

B. EXPERIMENT PROTOCOL

The experiment was conducted at least 1 hour after meal in a standard patient room with temperature kept at 25 °C. Specifically, each subject underwent a maximal stress test in supine posture in a bed with his/her feet putting on a bicycle ergometer. A mercury sphygmomanometer was connected to an automatic auscultative BP meter (GE Case 8000, Germany) by a Y-tube. The cuff BP was taken by a registered nurse every 2 minutes on the right arm of the subject. Continuous ECG and cardiac output (CO) were obtained by an impedance cardiographic device (Physio Flow PF-05, Macheren, France) from the subject's chest. Continuous BP was measured by Finometer (Finapres Medical System, Netherlands) from the left arm. Continuous PPG was acquired from the left index finger by using an in-house made acquisition device. Details of the specifications of the in-house system can be found in [19]. All data during the whole experiment were sampled at 1 kHz by a data acquisition system (DI220, DATAQ Instruments WinDaq, USA) and stored for further analysis.

After a 10-min rest, the bed was tilted towards the left-hand side of the subject by 20°–30° in order to avoid potential hypotension due to compression of the inferior vena cava. The subject was asked to start riding the bicycle at workload that began at 25W and increased by 25W every 2 minutes until it reached the tolerant limit of the subject. The workload was then kept at the tolerant limit until the subject reached his/her target heart rate (HR) [85% × (220 - Age)] or exhaustion. Then, the subject stopped riding and lie still on the bed to recover. The recovery phase lasted until CO returned to the baseline or at most for 15 min. The experimental protocol is presented in Figure 2.

The detailed protocol has been reported in [10]. Nonetheless, the subject pool included in this study was slightly different since subjects with Finapres BP failure or subjects whose PPG features cannot be extracted were excluded in the following analysis.

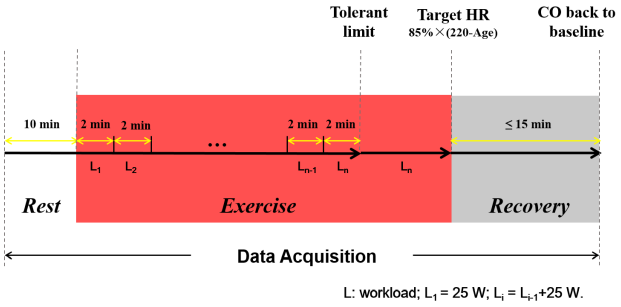

FIGURE 2. An overview of the experimental protocol.

C. SIGNAL PROCESSING

Continuous ECG, PPG and Finapres BP were used in this study. To remove noise and artifacts, the acquired ECG were filtered by a zero-phase low-pass filter with cutoff frequency at 30 Hz. PPG and Finapres BP were processed by the same type of low-pass filter at 16 Hz. The raw and filtered signals were presented in Figure 3. The 1st and 2nd derivatives of PPG were obtained by applying a finite impulse filter (FIR) differentiator on the PPG and 1st PPG derivative, respectively. Beat-to-beat SBP and DBP were extracted from the peaks and foots of Finapres BP respectively.

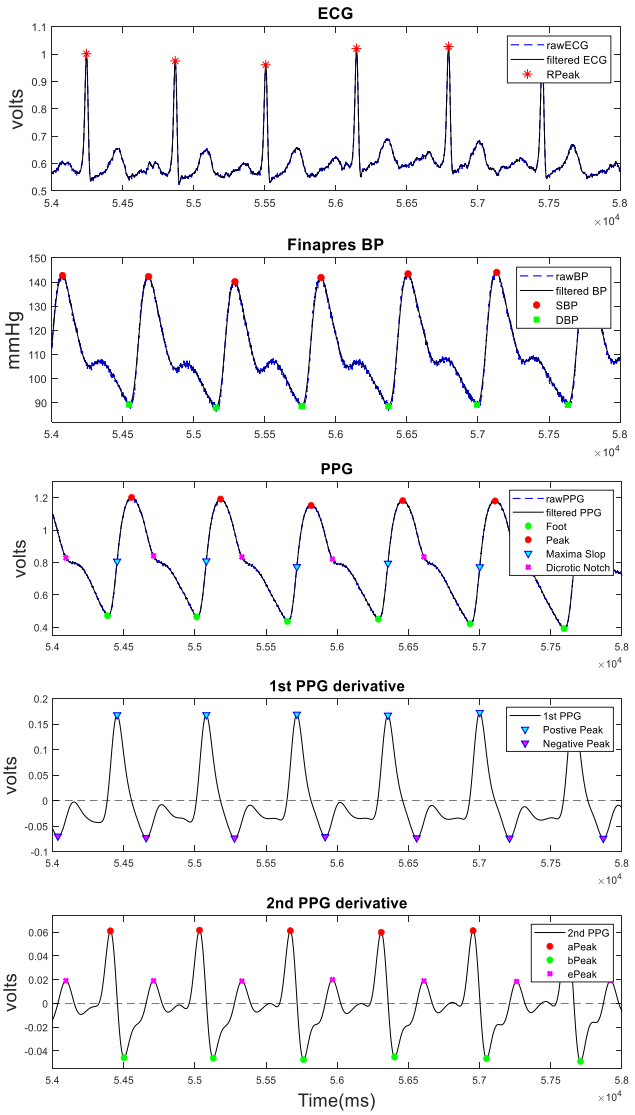

FIGURE 3. An illustration of the detection of the characteristics points on the physiological signal.

D. FEATURE EXTRACTION & SELECTION

The subjects were required to perform a lower body cycling exercise whilst signals were acquired from their chest and fingers simultaneously. The signal quality was generally good, but occasionally affected by motion. Therefore, the noisy episodes were manually removed after visual inspection. Outliers of each feature were also removed by thresholds. Around 72% of data were used in this study.

As shown in Figure 3 and 4, characteristic points of the waveforms of ECG, PPG, as well as the 1st & 2nd derivatives

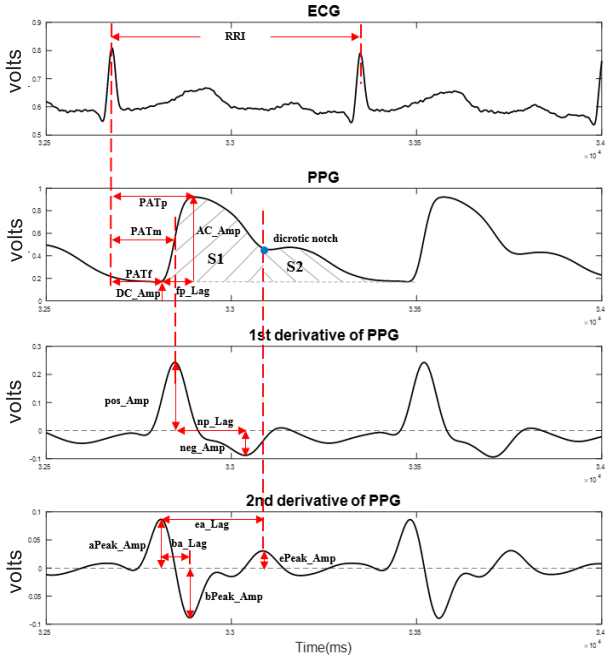

FIGURE 4. Definitions of the features extracted from electrocardiogram (ECG), photoplethysmogram (PPG) and the derivatives of PPG.

of PPG were identified, from which a set of features were calculated. The peaks of the 2nd derivative of PPG were extracted based on the definition in [20]. Peaks a and b were defined as the first peak and first valley of 2nd PPG derivative, and peak e was identified as the highest peak after peak b in the same cardiac circle. Peaks c and d, which were defined as the first peak and valley following peak b respectively [20], were unobvious in this dataset and hence were not used in this study.

SBP, DBP and all extracted features were averaged for every 10 non-overlapping beats of data. An additional feature – RRIV were calculated by the standard deviation (SD) of RRI of the 10 beats. To test the significance of features relating to BP, correlation analysis was performed between each extracted feature and SBP, DBP respectively. Features that had correlation with BP lower than 0.1 were discarded and were not used in further analysis. Five personal demographic parameters including age, weight, height, body mass index (BMI) and gender of subject were added in the feature set. As gender is a categorical parameter, it is defined as 1 for male and −1 for female. All selected features were then standardized to have zero mean and unit standard deviation before the next stage of analysis.

E. MACHINE LEARNING MODELS

Five ML regression methods were under investigation. Selected features served as inputs, while BP was considered as the targets. All algorithms were implemented in MATLAB.

- Multiple linear regression (MLR): MLR attempts to model the relationship between two or more variables and a response variable by fitting a linear equation to observed data. It has the advantage of displaying a weight for each feature showing its contribution [21].
- Regression tree (RT): RT is interpreted by building a tree structure. It sub-divides or partitions the space into small regions to deal with nonlinear and complex datasets. The problem is that they may create over-complex structures that do not generalize well 14].
- Ensemble of Trees (ETs): it is a model consisting of a weighted combination of multiple regression trees which aims to create a strong leaner by pulling together a set of weaker learners. Boosted and bagged methods were considered in this study.
- Support vector machine (SVM): SVM is one of the most powerful ML algorithms for its capability of creating strong models with reasonable training effort and high noise tolerance [14]. Different kernels including linear, quadratic, cubic and Gaussian functions were tested to obtain optimal performance.
- Gaussian Process Regression model (GPR): GPR is nonparametric kernel-based probabilistic model and has recently been evaluated in cuffless BP estimation task [15]. In this study, 4 kernel functions: rational quadratic, squared exponential, Matern 5/2 and exponential functions were investigated in the study.

Five-fold cross validation was used to test the performance of the above regression models. Specifically, all data points were randomly divided into 5 equal folds. For each regression method, a model was built on 4-folds of data and tested in the remaining 1-fold of data. The process was iterated for 5 times and the averaged results were reported. To avoid possibly overfitting the training data in each fold, a heuristic procedure was adopted to determine the hyperparameters of each model [22]. Figure 5 shows the workflow of the study.

Unpaired student's t-test was employed to test the significance of differences in physical parameters between the two groups in Table 1. The mean absolute error (MAE), mean error (ME), standard deviation (SD), as well as squared correlations (r^2) between reference and estimated BP were used as metrics for evaluating the different models.

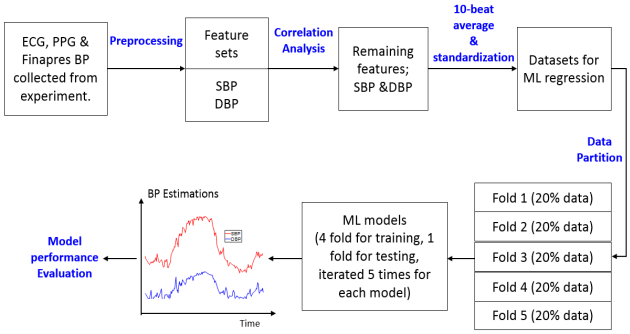

FIGURE 5. A block diagram of the workflow of the study.

TABLE 1. Demographic description of all subjects.

	Healthy	Risk Factor	CVD
No. of subjects (Male/Female)	22 (16/6)	16 (9/7)	24 (22/2)
Age (years)	60±8	57±14	61±10
Height (cm)	164.4±8.5	161.6±12.1	161.8±8.2
Weight (kg)	63.0±8.7	69.6±23.3	69.8±14.7
BMI (kg/m^2)	23.3±2.2	26.1±5.8	26.5±4.3**
Rest SBP (mmHg)	134±20	138±16	136±18
Rest DBP (mmHg)	78±10	78±11	81±11

BMI: body mass index; SBP: systolic BP; DBP: diastolic BP;
**: indicates P < 0.01 between Healthy and CVD group.

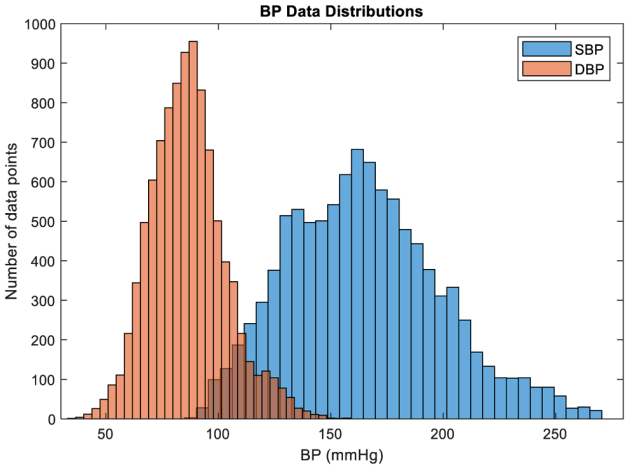

FIGURE 6. Data distribution for SBP and DBP.

III. RESULTS

Table 1 summarizes the demographic characteristics of the sub-groups of subjects. There were no significant differences in age, height, weight and resting SBP & DBP between the three subject groups while BMI was significantly larger in the CVD patients than in the healthy subjects.

The average length of recording for each subject was 35 minutes. Average time taken for reaching target HR since the start of exercise was 16.5 minutes, and average duration of recovery was 13.8 minutes. The BP ranges were 75-280 mmHg for SBP and 36-157 mmHg for DBP respectively. Totally 101,270 beats of data were collected from all subjects. The distributions of the 10-beat averaged SBP and DBP were shown in Figure 6. Details of the features and correlation between each feature and SBP and DBP were listed in Table 2. Two features (e_aR and ea_Lag) were discarded for the estimation of SBP and three features (DC_Amp, fp_Lag and ba_Lag) were discarded for the estimation of DBP due to their low correlations with SBP and DBP respectively. Therefore, 20 and 19 features were used for SBP and DBP regression respectively.

Table 3 compares the performance of the 5 models in estimating SBP with the criteria set out by the AAMI standard. ''Gaussian'' and ''rational quadratic'' kernel worked best

TABLE 2. Description of features extracted from ECG, PPG and 1st & 2nd derivatives.

Sources	Feature	Definition	Correlation with SBP	Correlation with DBP
ECG	RRI	Interval between R peaks of two consecutive ECG waveforms	-0.30	-0.36
	RRIV	Standard deviation of RRI of 10 beats	-0.13	-0.12
ECG & PPG	PATp	Interval between ECG R peak and peak of PPG in the same cardiac cycle	-0.23	-0.25
	PATm	Interval between ECG R peak and peak of 1st PPG derivative in the same cardiac cycle	-0.51	-0.27
	PATf	Interval between ECG R peak and foot of PPG in the same cardiac cycle	-0.52	-0.15
PPG	DC_Amp	Amplitude of DC component	0.20	0.09
	AC_Amp	Amplitude of AC component	-0.41	-0.36
	PIR	Photoplethysmogram intensity ratio: the ratio of the PPG peak intensity to PPG valley intensity of one cardiac cycle as defined in [20].	-0.24	-0.15
	AreaR	S2/S1; S1: shaded area between foot and the dicrotic notch of PPG; S2: shaded area between dicrotic notch and foot of next beat of PPG	-0.25	-0.14
	fp_Lag	Interval between foot and peak of PPG	0.11	0.00
1st PPG derivative	pos_Amp	Amplitude of the most positive peak of 1st PPG derivative	-0.41	-0.37
	neg_Amp	Amplitude of the moat negative valley of 1st PPG derivative	-0.34	-0.27
	np_Lag	Interval between most positive peak and most negative valley of 1st PPG	0.14	-0.12
2nd PPG derivative	b_aR	Ratio between amplitude of b and a peak of 2nd PPG	-0.33	-0.19
	e_aR	Ratio between amplitude of e and a peak of 2nd PPG	0.03	0.18
	ba_Lag	Interval between b and a peak of 2nd PPG	-0.20	-0.09
	ea_Lag	Interval between e and a peak of 2nd PPG	0.04	-0.21

TABLE 3. ***Performance of the 5 models in estimating SBP and DBP.***

	SBP			DBP		
	MAE	ME ± SD	r^2	MAE	ME ± SD	r^2
MLR	17.6	0.0 ± 22.7	0.56	9.7	0.0 ± 12.6	0.42
RT	7.9	0.1 ± 12.1	0.87	4.9	-0.0 ± 7.2	0.82
ETs	6.9	-0.0 ± 9.8	0.92	4.3	-0.0 ± 6.1	0.87
SVM	6.1	-0.1 ± 9.3	0.93	4.0	0.2 ± 5.8	0.88
GPR	4.8	0.0 ± 6.9	0.96	3.4	0.0 ± 4.9	0.91
AAMI standard	-	≤5 ± 8	-	-	≤5 ± 8	-

Remark: units for MAE, ME and SD are mmHg.

for SVM and GPR model respectively. "Bagged" method showed better results than "Boosted" method for the ETs model. The MAE, ME, and SD of the estimation differences, as well as the squared correlations between the estimated and reference BP were presented. GPR model achieved the lowest MAE and SD, as well as the highest correlation between the estimated and reference values for both SBP and DBP.

Bland-Altman plots and scatter plots for GPR model were shown in Figure 7. Figure 8 shows the evaluation of the GPR model under the IEEE standard for wearable cuffless blood pressure measuring devices (IEEE Standard P1708) [23]. Absolute mean differences vs. standard deviation of differences between the reference and estimated BP were shown for each subject. Figure 9 shows the best case and the worst case scenarios for the estimation of SBP by the GPR model.

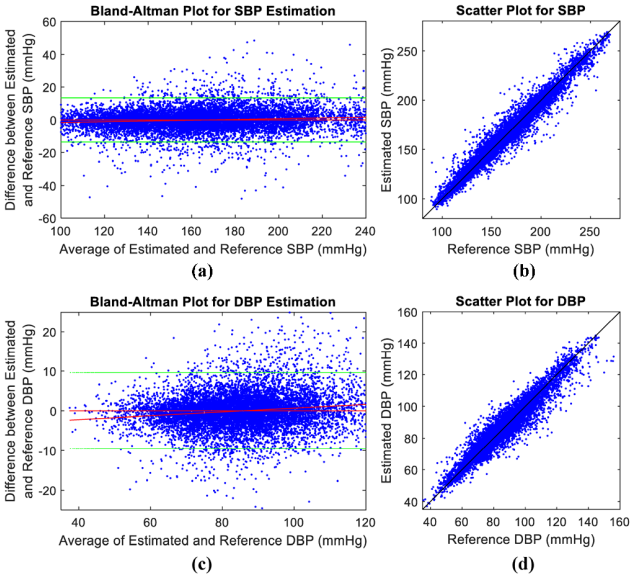

FIGURE 7. **(a) Bland-Altman plot and (b) Scatter plot for the estimation of SBP by the GPR model. (b) Bland-Altman plot and (b) Scatter plot for the estimation of DBP by the GPR model.**

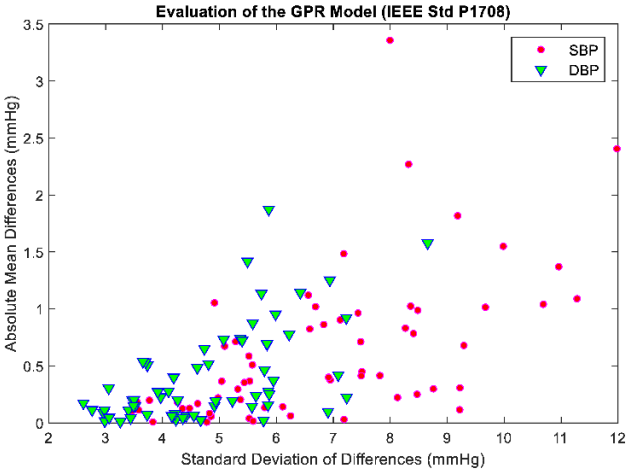

FIGURE 8. **The mean differences vs. standard deviation of differences between BP estimated by the GPR model and the reference BP of each subject. The graphical representation is one way of plotting the measurement differences according to the IEEE Standard on cuffless wearable blood pressure measuring devices (P1708).**

IV. DISCUSSION

Continuous and ubiquitous BP measurement has been a popular research topic for the last two decades. PTT/PWV based approaches enable cuff-less and wearable measurement of BP. Most of the previous studies focused on deriving the

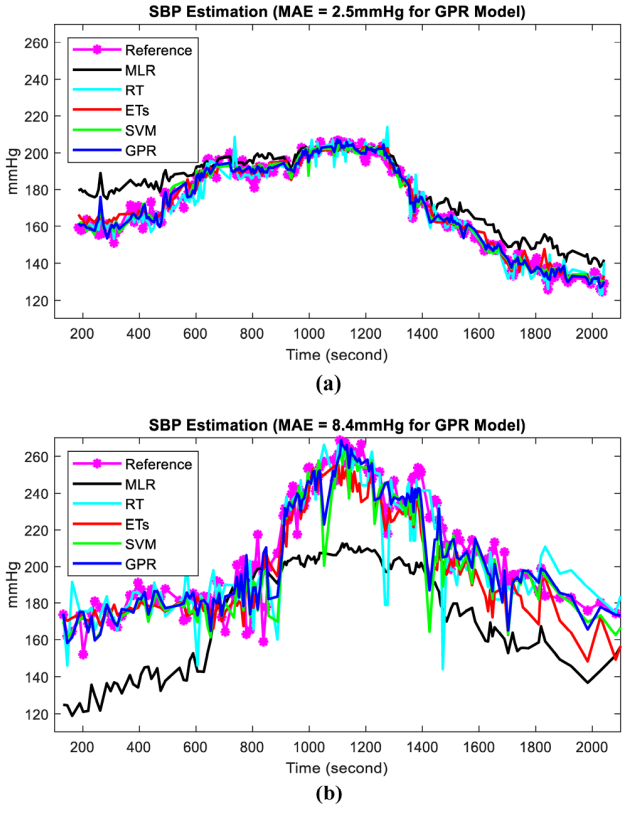

FIGURE 9. **Typical time series examples of SBP estimations from different models. (a) subject of smallest MAE with GPR model; (b) subject of largest MAE with GPR model.**

mathematical models between PTT and BP, and estimating BP mainly from PTT.

Nevertheless, the PTT-BP relationship exhibits high non-linearity and complexity [10]. Influences of confounding factors such as PEP and vascular tone must be taken into account in order to ensure accurate measurement in dynamic situations. Under these situations, the traditional mechanism-based models are insufficient to describe the complex system and realize reliable BP estimation. Due to the increasingly powerful computational resources, data-driven cuff-less BP measurement based on ML techniques as presented in this study is achievable nowadays. Beats-to-beats estimation of BP without a cuff is possible.

A. ML BASED CUFFLESS BP ESTIMATION DURING EXERCISE

Different ML techniques have been studied for estimating cuffless BP from ECG and/or PPG sensor features, including regularized linear regression [14], decision tree regression [14], and adaptive boosting [14], ridge linear regression [16], multilayer perceptron neural network [16], SVM [14], [16], random forest [14],]16], Deep Belief Network [24], and artificial neural network (ANN) [17]. These studies attempted to estimate BP using data collected either from subjects under relatively stable conditions in caring centers of hospitals [16], [24] or from a public physiological database (i.e. MIMIC II) [14], [17].

Measuring BP during exercise is challenging but important, as exercise can be an important trigger of cardiovascular events. Moreover, accurate and continuous tracking of BP in dynamic conditions can provide novel opportunities for research and clinical assessment [25]. Studies that examined ML-based continuous BP estimation during exercise were few. One study [26] examined cuffless BP estimation before and after rope skipping exercise using MLR and SVM; however, the accuracy was low during follow-up experiments. Another study [21] estimated cuffless SBP by MLR during physical exercise, using PPG and ECG sensor features collected at rest for calibration. Both studies were conducted on healthy young subjects with exercise intensities that were much smaller than our study. To our best knowledge, our work is the first study to investigate ML-based approaches for the continuous beats-to-beats estimation of cuffless BP during physical exercise on a general elderly population. These subjects were more susceptible to develop cardiovascular events than the healthy, young subjects when their cardiovascular system were stressed.

B. CHALLENGES IN THE EXTRACTION OF PPG FEATURES

PPG contour analysis provides valuable information about the cardiovascular system. For example, time interval and amplitude ratio between the first and second PPG peaks are related to arterial properties and vasomotor tone [13], [27]. PPG AC amplitude is determined by the cardiac synchronous changes in the blood volume with each heartbeat, while its DC amplitude is influenced by respiration, sympathetic nervous system activity and thermoregulation. Both parameters were able to partly reflect the regulation of the cardiovascular system during exercise. On the other hand, the PPG waveform is also affected by temperature and sensor-contact force [28]. In this study, PPG signal was collected from the subjects' finger which was kept still during the experiment in order to minimize the influence of contact force. Finger temperature reflected thermoregulation, which is weakly related to SBP [29] and confirmed in the correlation analysis shown in Table 2.

Features related to the second peak of PPG were not included in this study in spite of their physiological meaning. We observed that the PPG morphology evolved along with the progression of graded exercise. The PPG waveforms of the same subject have either one significant peak, multiple peaks or no obvious peak at diastole during different phases of exercise. In fact, it is well accepted that PPG includes three elements, i.e., main forwarding wave and two reflection waves, i.e. a tidal wave and a dicrotic wave. The observation may due to the unnoticeable first reflection wave and highlighted second reflection wave, and reduced PWV caused by muscle vasodilation and decreased muscle vascular resistance during exercise in response to increased demand of oxygen and other nutrients for muscle. Meanwhile, motion artifacts may also contribute to the phenomenon. Therefore, only features from PPG and its derivatives that were relatively stable and robust during the whole process were used.

Around 28% of data were discarded due to waveform distortions caused by motion in one of the signals, revealing challenges of feature extraction in such a condition. To address this question, sensor design and other features that represent the waveform, such as PPG spectral characteristics, can be investigated in the future. Other methods such as a genetic algorithm-based feature selection method can also help in identifying the most appropriate features for cuffless BP estimation [26].

C. POTENTIAL OF THE PROBABILISTIC NONPARAMETRIC MODEL

Five ML regression models were investigated in this work. The performance of MLR, RT and ETs were unsatisfactory, indicating that the relationship between BP and the wearable sensor features were non-linear. The differences between the reference and estimated DBP using RT, ETs, SVM were within 5 ± 8 mmHg; however, the estimation differences were above 5 ± 8 mmHg for the estimation of SBP using these models. On the other hand, the probabilistic nonparametric GPR model fully complied with the AAMI standard in terms of both ME and SD and also outperformed the other four models in terms of MAE for the estimation of both SBP and DBP. In fact, GPR can be interpreted as a Bayesian version of SVM. It is therefore not surprising that SVM with Gaussian kernel obtained the second best results in this study. Specifically, being a probabilistic nonparametric ML approach, GPR did not attempt to fit the data by using a fixed class of function. GPR can avoid errors induced by

the inappropriate assumption on the underlying functions used by the parametric methods like MLR or SVM with linear kernels. Instead, GPR considers an infinite number of functions by assuming a *prior* over them. As practical problems normally ask only for properties of functions at a finite number of data points, GPR is computationally tractable. Moreover, GPR presents great flexibility in the functions when additional observation arrives [30].

D. FUTURE WORK

Five-fold cross validation method was used in this study. In the future, the leave-one-subject-out cross validation can be tested when the subject pool is increased and personalized calibration methods are employed. Moreover, follow-up studies are required to confirm whether personalized calibration will further reduce the estimation differences and whether these training weights can hold valid for a longer period than previous studies [19].

The results of this study showed that the probabilistic nonparametric GPR model can better described the inherent complex relationship between BP and the selected wearable sensor features. The GPR model has great potential for developing future cuffless BP estimation systems.

V. CONCLUSION

The main objective of this study is to evaluate five ML techniques in modeling the complex relationship of BP and wearable sensor features during supine cycling exercise in a cohort of elderly subjects. The results suggested that the probabilistic nonparametric GPR method has the potential to describe this relationship and achieve an estimation difference that is acceptable by both the AAMI and IEEE Standard for BP measuring devices. The estimation differences (MAE, ME $\pm$ SD) for the GPR models were (4.8, 0.0 $\pm$ 6.9 mmHg) and (3.4, 0.0 $\pm$ 4.9 mmHg) for the 10-beat SBP and DBP averages, respectively. None of the other four methods can model the estimation of SBP to an estimation difference that is acceptable by the AAMI or IEEE Standard. The work is fundamental for the future development of cuffless BP estimation systems, particularly in selecting the optimal estimation models for these devices.

ACKNOWLEDGMENT

The authors would like to thank Dr. Bryan P. Yan and Dr. Cheuk-Man Yu, Division of Cardiology, Prince of Wales Hospital, The Chinese University of Hong Kong, for their help in collecting the patient data used in this study.

REFERENCES

[1] S. R. Steinhubl, E. D. Muse, P. M. Barrett, and E. J. Topol, "Off the cuff: Rebooting blood pressure treatment," *Lancet*, vol. 388, no. 10046, p. 749, Aug. 2016.

[2] C. K. Chow, K. K. Teo, S. Rangarajan, S. Islam, and R. Gupta, "Prevalence, awareness, treatment, and control of hypertension in rural and urban communities in high-, middle-, and low-income countries," *JAMA*, vol. 310, no. 9, pp. 959–968, 2013.

[3] T. SPRINT Research Group, "A randomized trial of intensive versus standard blood-pressure control," *New England J. Med.*, vol. 373, no. 22, pp. 2103–2116, Nov. 2015.

[4] R. Mukkamala, J.-O. Hahn, O. T. Inan, L. K. Mestha, C.-S. Kim, and H. Töreyin, "Toward ubiquitous blood pressure monitoring via pulse transit time: Theory and practice," *IEEE Trans. Biomed. Eng.*, vol. 62, no. 8, pp. 1879–1901, Aug. 2015.

[5] A. Chandrasekhar, C.-S. Kim, M. Naji, K. Natarajan, J.-O. Hahn, and R. Mukkamala, "Smartphone-based blood pressure monitoring via the oscillometric finger-pressing method," *Sci. Transl. Med.*, vol. 10, no. 431, Mar. 2018, Art. no. eaap8674.

[6] C. C. Y. Poon and Y. T. Zhang, "Cuff-less and noninvasive measurements of arterial blood pressure by pulse transit time," in *Proc. IEEE Eng. Med. Biol. 27th Annu. Conf.*, Jan. 2006, pp. 5877–5880.

[7] R. A. Payne, C. N. Symeonides, D. J. Webb, and S. R. J. Maxwell, "Pulse transit time measured from the ECG: An unreliable marker of beat-to-beat blood pressure," *J. Appl. Physiol.*, vol. 100, no. 1, pp. 136–141, 2006.

[8] C. S. Kim, A. M. Carek, R. Mukkamala, O. T. Inan, and J. O. Hahn, "Ballistocardiogram as proximal timing reference for pulse transit time measurement: Potential for cuffless blood pressure monitoring," *IEEE Trans. Biomed. Eng.*, vol. 62, no. 11, pp. 2657–2664, Nov. 2015.

[9] Y. Zheng, C. C. Y. Poon, B. P. Yan, and J. Y. W. Lau, "Pulse arrival time based cuff-less and 24-H wearable blood pressure monitoring and its diagnostic value in hypertension," *J. Med. Syst.*, vol. 40, no. 9, p. 195, Sep. 2016.

[10] Q. Liu, B. P. Yan, C.-M. Yu, Y.-T. Zhang, and C. C. Y. Poon, "Attenuation of systolic blood pressure and pulse transit time hysteresis during exercise and recovery in cardiovascular patients," *IEEE Trans. Biomed. Eng.*, vol. 61, no. 2, pp. 346–352, Feb. 2014.

[11] Y. Ma, J. Choi, A. Hourlier-Fargette, Y. Xue, H. U. Chung, and J. Y. Lee, "Relation between blood pressure and pulse wave velocity for human arteries," *Proc. Nat. Acad. Sci. USA*, vol. 115, no. 44, pp. 11144–11149, 2018.

[12] J. A. Pandit, E. Lores, and D. Batlle, "Cuffless blood pressure monitoring: Promises and challenges," *Clin. J. Amer. Soc. Nephrol.*, vol. 15, no. 10, pp. 1531–1538, 2020.

[13] J. Allen, "Photoplethysmography and its application in clinical physiological measurement," *Physiol. Meas.*, vol. 28, no. 3, pp. R1–R39, Mar. 2007.

[14] M. Kachuee, M. M. Kiani, H. Mohammadzade, and M. Shabany, "Cuffless blood pressure estimation algorithms for continuous healthcare monitoring," *IEEE Trans. Biomed. Eng.*, vol. 64, no. 4, pp. 859–869, Apr. 2017.

[15] M. H. Chowdhury, M. N. I. Shuzan, M. E. H. Chowdhury, Z. B. Mahbub, M. M. Uddin, A. Khandakar, and M. B. I. Reaz, "Estimating blood pressure from the photoplethysmogram signal and demographic features using machine learning techniques," *Sensors*, vol. 20, no. 11, p. 3127, Jun. 2020.

[16] E. Monte-Moreno, "Non-invasive estimate of blood glucose and blood pressure from a photoplethysmograph by means of machine learning techniques," *Artif. Intell. Med.*, vol. 53, no. 2, pp. 127–138, Oct. 2011.

[17] X. Xing and M. Sun, "Optical blood pressure estimation with photoplethysmography and FFT-based neural networks," *Biomed. Opt. Exp.*, vol. 7, no. 8, pp. 3007–3020, Aug. 2016.

[18] K. Kario, "Management of hypertension in the digital era: Small wearable monitoring devices for remote blood pressure monitoring," *Hypertension*, vol. 76, no. 3, pp. 640–650, 2020.

[19] M. Y.-M. Wong, C. C.-Y. Poon, and Y.-T. Zhang, "An evaluation of the cuffless blood pressure estimation based on pulse transit time technique: A half year study on normotensive subjects," *Cardiovascular Eng.*, vol. 9, no. 1, pp. 32–38, 2009.

[20] S. C. Millasseau, J. M. Ritter, K. Takazawa, and P. J. Chowienczyk, "Contour analysis of the photoplethysmographic pulse measured at the finger," *J. Hypertension*, vol. 24, no. 8, pp. 1449–1456, Aug. 2006.

[21] S. Sun, R. Bezemer, X. Long, J. Muehlsteff, and R. Aarts, "Systolic blood pressure estimation using PPG and ECG during physical exercise," *Physiol. Meas.*, vol. 37, no. 12, p. 2154, 2016.

[22] *Applied Machine Learning, Part 3: Hyperparameter Optimization*. Accessed: Aug. 16, 2021. [Online]. Available: https://www.mathworks.com/videos/applied-machine-learning-part-3-hyperparameter-optimization-1547849445386.html

[23] *IEEE Standard for Wearable Cuffless Blood Pressure Measuring Devices*, IEEE Standard 1708-2014, 2014.

[24] J. C. Ruiz-Rodríguez, A. Ruiz-Sanmartín, V. Ribas, J. Caballero, A. García-Roche, J. Riera, X. Nuvials, M. de Nadal, O. de Sola-Morales, J. Serra, and J. Rello, "Innovative continuous non-invasive cuffless blood pressure monitoring based on photoplethysmography technology," *Intensive Care Med.*, vol. 39, no. 9, pp. 1618–1625, Sep. 2013.

[25] T. Wibmer, K. Doering, C. Kropf-Sanchen, S. Rüdiger, I. Blanta, K. M. Stoiber, W. Rottbauer, and C. Schumann, "Pulse transit time and blood pressure during cardiopulmonary exercise tests," *Physiol. Res.*, vol. 63, no. 3, pp. 287–296, 2014.

[26] F. Miao, N. Fu, Y.-T. Zhang, X.-R. Ding, X. Hong, and Q. Y. He, "A novel continuous blood pressure estimation approach based on data mining techniques," *IEEE J. Biomed. Health Inform.*, vol. 21, no. 6, pp. 1730–1740, Nov. 2017.

[27] X.-R. Ding, Y.-T. Zhang, J. Liu, W.-X. Dai, and H. K. Tsang, "Continuous cuffless blood pressure estimation using pulse transit time and photoplethysmogram intensity ratio," *IEEE Trans. Biomed. Eng.*, vol. 63, no. 5, pp. 964–972, May 2016.

[28] Y. Sun and N. Thakor, "Photoplethysmography revisited: From contact to noncontact, from point to imaging," *IEEE Trans. Biomed. Eng.*, vol. 63, no. 3, pp. 463–477, Mar. 2016.

[29] P. Franklin, D. Green, and N. Cable, "The influence of thermoregulatory mechanisms on post-exercise hypotension in humans," *J. Physiol.*, vol. 470, no. 1, pp. 231–241, 1993.

[30] C. E. Rasmussen and C. K. I. Williams, *Gaussian Processes in Machine Learning*. Cambridge, MA, USA: MIT Press, 2006.

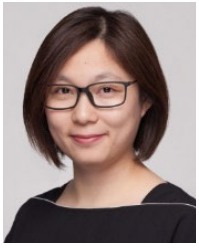

QING LIU (Member, IEEE) received the B.E. degree in automation from the University of Science and Technology of China, Hefei, China, in 2008, and the Ph.D. degree in electronic engineering from the Chinese University of Hong Kong, Shatin, N.T., Hong Kong, in 2013.

From 2015 to 2017, she was a Postdoctoral Fellow with Suzhou Institute of Biomedical Engineering and Technology, The Chinese Academy of Science. She joined Xi'an-Jiaotong Liverpool University (XJTLU), Suzhou, Jiangsu, China, in 2018. She is currently an Assistant Professor with the Department of Communications and Networking, School of Advanced Technology, XJTLU. Her research interests include unobtrusive sensing and wearable devices, health informatics, and physiological modeling.

Dr. Liu is an Affiliated Member of IEEE-EMBS Wearable Biomedical Sensors and Systems Technical Committee. She served as the Technical Program Committee Member for the 16th and 17th IEEE International Conference on Wearable and Implantable Body Sensor Networks (BSN'19 and BSN'21).

YALI ZHENG (Member, IEEE) received the Ph.D. degree in electronic engineering from the Chinese University of Hong Kong, in 2014. From 2014 to 2018, she was a Postdoctoral Fellow with the Department of Surgery, Faculty of Medicine, The Chinese University of Hong Kong. She is currently an Assistant Professor with the Department of Biomedical Engineering, Shenzhen Technology University, Shenzhen, China. She has published more than 30 scientific papers in the area of biomedical engineering. Her research interests include wearable medical devices and biomedical and health data analytics.

Dr. Zheng is an Affiliated Member of IEEE-EMBS Wearable Biomedical Sensors and Systems Technical Committee, and the Executive Committee Member of IEEE EMB Hong Kong–Macau Joint Chapter. The Google citations of her work are > 1400 times and her recent H-index is 13. She also served as the Technical Program Committee member for the 16th and 17th IEEE International Conference on Wearable and Implantable Body Sensor Networks (BSN'19 and BSN'21).

YUANTING ZHANG (Fellow, IEEE) received the bachelor's and master's degrees from Shandong University, Shandong, China, in 1976 and 1981, respectively, and the Ph.D. degree in electrical and computer engineering from the University of New Brunswick, Fredericton, Canada, in 1990.

He is currently the Chair Professor of biomedical engineering with the Department of Mechanical and Biomedical Engineering, City University of Hong Kong. He was the Founding Director of the Key Laboratory for Health Informatics of the Chinese Academy of Sciences (CAS), and the Founding Director of the CAS-SIAT Institute of Biomedical and Health Engineering. From 1994 to 2015, he dedicated his service to the Department of Electronic Engineering, Chinese University of Hong Kong (CUHK). He was the Sensing System Architect in sensing hardware and health technology at Apple Inc., Cupertino, CA, USA. Before joining the CUHK, he was a Research Associate and an Adjunct Assistant Professor, from 1989 to 1994, with the University of Calgary, Canada. His research interests include cardiovascular health informatics, unobtrusive sensing and wearable devices, BSN/BAN security, neural muscular modeling, and pHealth technologies.

Prof. Zhang is a member of the Fellow Membership Committee and Award Committee of the International Academy of Medical and Biological Engineering (IAMBE). He was the Editor-in-Chief for IEEE TRANSACTIONS ON INFORMATION TECHNOLOGY IN BIOMEDICINE and the founding Editor-in-Chief of IEEE JOURNAL OF BIOMEDICAL AND HEALTH INFORMATICS. He currently serves as the Editor-in-Chief for *IEEE Reviews in Biomedical Engineering*, the Chair of 2018 Gordon Research Conference on Advanced Health Informatics, the Chair of the Working Group for the development of IEEE Standard on Wearable Cuffless Blood Pressure Measuring Devices (IEEE 1708), the Chair of 2016–2018 IEEE Award Committee in biomedical engineering.

CARMEN C. Y. POON (Senior Member, IEEE) received the B.A.Sc. degree in engineering science and the M.A.Sc. degree in biomaterials and biomedical engineering and electrical and computer engineering from the University of Toronto, and the Ph.D. degree in electronic engineering from The Chinese University of Hong Kong (CU).

She was an Assistant Professor with the Department of Surgery, CU Medicine. Her research interest includes informatics that have the potential to change surgical practices. Several pieces of her works in these areas have been rated *Highly Cited Papers* by *ISI Web of Science* (2015–2021), and collectively, her works have been cited >3800 times in Scopus until June 2021. She was a Distinguished Lecturer of EMBS (2019–2020) and is currently the Director of GMed IT Ltd.

Dr. Poon received the Distinguished Service Award for serving as the Managing Editor for IEEE JOURNAL OF BIOMEDICAL AND HEALTH INFORMATICS (2009–2016). She is currently an Editorial Board Member for several international peer-reviewed journals published by IEEE, IOP, Elsevier, and ACM. She received the IFMBE/IAMBE Early Career Award from the International Federation of Medical and Biological Engineering/The International Academy of Medical and Biological Engineering in 2015, and the IEEE-EMBS Academic Early Career Achievement Award in 2018. She serves as the Chair of the IEEE Biomedical Engineering Award Committee (2021–2022) and was the Conference Chair of the 16th International Conference on Wearable and Implantable Body Sensor Networks in 2019, the Chair of the Technical Committee on Wearable Biomedical Sensors and Systems of the IEEE Engineering in Medicine and Biology Society (EMBS) (2016–2017), and an EMBS Administrative Committee Member (2014–2016).